

JAOUEN Rachel<sup>1,2</sup>  
MARTINEAU Jean-Pierre<sup>1</sup>  
DAMAY Thomas<sup>1</sup>  
HASCOET Jean-Yves<sup>2</sup>

## **A NEW MULTIDISCIPLINARY APPROACH FOR THREE-DIMENSIONAL FOIL MACHINING**

The context of this paper implies disciplines of mechanical design, machining and hydrodynamics behaviours applied to propellers. Performances of propellers are linked with their shape and their surface texture. To optimise hydrodynamics behaviours, it is demonstrated in this paper that required polishing operation is not essential. To study the influence of an predefined surface texture on the performances of a three-dimensional foil, a comparative analysis is conducted. The presented methodology allows the definition of tool paths, according to the desired surface texture and upstream flow. Three foils are machined, and their performances are compared to each other: the first, considered as the reference, has a surface roughness like mirror, the second features machined peaks parallel to the upstream flow and the third has machined peaks following streamlines obtained by Computational Fluid Dynamics for operating conditions. The validation of this method is experimental: on the one hand by the manufacturing of foils following pre-established trajectories, and on the other hand by the functional test in hydrodynamic tunnel. This paper presents the methodology steps, and the hydrodynamic behaviours that the three different foils show. In a first approach, the different surface textures do not influence the lift coefficient but strongly influence the drag coefficient of a foil. Furthermore several hypotheses educed from the observed tendencies are discussed.

### **1. INTRODUCTION**

The conception of marine propeller implies knowledge and know-how in several disciplinary fields, in particular in hydrodynamics and manufacturing. Their design is strongly linked to stringent constraints such as a smooth surface texture, since propeller performances are linked with their shape and surface texture characteristics. Nowadays, marine propellers are usually manufactured both by moulding and by machining. These two manufacturing processes are generally followed by a long and expensive hand polishing operation because propeller designers impose a mirror surface[1]. The purpose of this study

---

<sup>1</sup> Institut de Recherche de l'Ecole Navale, BCRM , ENGEP Ecole, Marine nationale, CC 600, 29240 BREST Cedex 9, France, [rachel.jaouen@ecole-navale.fr](mailto:rachel.jaouen@ecole-navale.fr), [jean-pierre.martineau@ecole-navale.fr](mailto:jean-pierre.martineau@ecole-navale.fr) , [thomas.damay@ecole-navale.fr](mailto:thomas.damay@ecole-navale.fr)

<sup>2</sup> Institut de Recherche en Communication et Cybernétique de Nantes, 1 rue de la Noë, BP 92101, 44321 Nantes Cedex 03, France, [rachel.jaouen@ircyn.ec-nantes.fr](mailto:rachel.jaouen@ircyn.ec-nantes.fr), [jean-yves.hascoet@ircyn.ec-nantes.fr](mailto:jean-yves.hascoet@ircyn.ec-nantes.fr)

is first to determine how machining peaks and their organization influence propeller hydrodynamic performances. We also aim at optimizing the machining tool paths due to the variation of the hydrodynamic performances. This study is based on previous works[2] in which, concerning two-dimensional foils, the influence of the machined surface texture on the hydrodynamic performances was reaserched. Machining peak height and organization, perpendicular or parallel to the upstream flow, were studied . The work presented in this paper extends the study to the manufacturing of three-dimensional foils.

To determine the influence of an preset surface texture on the hydrodynamic performances of three-dimensional foils, a comparative analysis is performed. First, three foils, whose surface textures are different, are manufactured: foil with a surface like a mirror, a foil with machining peaks parallel to the upstream flow and a foil with machining peaks following streamlines obtained by Computational Fluid Dynamics (CFD) simulations for operating conditions. To manufacture an organised surface texture, a new methodology is developed to obtain each foil. Then the dimensional characteristics are controlled and the hydrodynamic performances of these foils are measured in a tunnel.

The first part of this paper highlights the context of the study. Then an innovative methodology of the tool paths generation of foils is described. Next the foil machining is presented. In the third part, the machining of the foils is described in detail. Finally hydrodynamic tests are described and the three analysis are presented and compared to each other.

## 2. CONTEXT OF THE STUDY

The energy consumption of a ship are directly linked to their propulsive system. The degradation of a propeller surface texture directly increases its fuel consumption [3]. In particular, the roughness located on the leading edge and foil tip is a determining factor regarding the decrease of performances. In these locations, the surface texture must be as smooth as possible. The constant roughness distribution is usually applied to both faces of the foil, even though the surface texture of the pressure side influences less the propulsive driving behaviour than the suction side. This is probably due to the generation of the lift effect: a depression and high velocities on the suction side combined with an overpressure and low velocities on the pressure side. Consequently it is possible to define different levels of surface roughness for the pressure side and the suction side. It is interesting to note that ISO standards for propeller manufacturing do not take into account a possible variation of the quality of the surface texture [4]. Standards are restricted to a single value of roughness all over the blade.

The study of the influence of an organised surface texture on two-dimensional foils shows that the foil whose machining peaks are parallel to the upstream flow allows to improve the hydrodynamic performances in relation to the foil whose machining peaks are transverse to the upstream flow [5]. Moreover, this study shows that there is no influence of the machining peak height on the hydrodynamic performances.

From these observations, a methodology, allowing the machining trajectory generation, is developed to obtain predefined surface textures.

### 3. METHODOLOGY

In order to evaluate the influence of an predefined surface texture on the performances of a three-dimensional lifting body, a comparative experimental study is implemented. The comparison concerns the obtained hydrodynamic performances with three manufactured foils. An original methodology is elaborated to machine the three foils taking into account their hydrodynamics and manufacturing constraints. The described method allows the generation of trajectories for the machining of the third foil, whose machining peaks that follow the streamlines whose achievement is the most delicate. Nevertheless this method consists of several stages allowing to generate trajectories for the first and the second foils, which are only geometrically defined.

First, the general geometry of the reference foil is chosen. To prepare the manufacturing of the second and the third foil, a distribution of the tool path's distance is calculated. The purpose of this computation is to manufacture a constant machining peaks at constant height at the leading edge of the foil. Then, to machine the third foil, the fluid velocity field is computed around the foil to simulate and compute the streamlines. The Computational Fluid Dynamics software allows to obtain streamlines at the close vicinity of the foil. Finally these streamlines are used to define the needed trajectories

#### 3.1. GENERAL GEOMETRY OF THE FOIL

In this study, the chosen foil is an elliptic shaped wing with a straight trailing edge (Fig. 1) whose basic section is a NACA0015. This section corresponds to a symmetric section in which the maximal thickness is equal to 15 % of the chord. The maximal thickness is located at 30 % from the leading edge (Fig.2). One of the interesting theoretical characteristics of this type of section is the fact that the lift coefficient value is equal to zero for a incidence angle of  $0^\circ$ . The choice of this shape type is justified by the fact that the three-dimensional hydrodynamic effects are maximized on this type of wing [6].

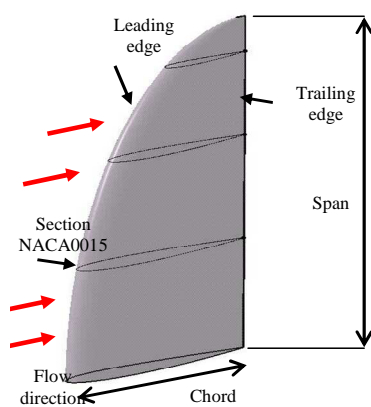


Fig. 1. General geometry of the foil

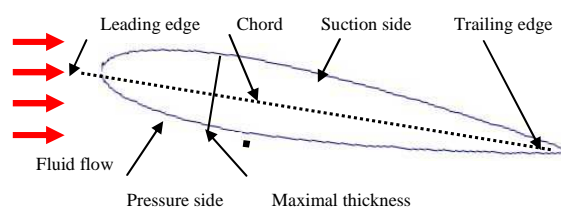


Fig. 2. Description of the basic section NACA0015

### 3.2. CHOICES RELATED TO MANUFACTURING

Due to the foil geometry, 5 axis milling has to be chosen to manufacture the parts. Instead of classical tool trajectories [7], the global orientation of the tool paths will take into account the simulated fluid's flow direction. Moreover, the whole surface will be machined with no recovery zone – ie the tool does not ever back in the same area of the surface- using a ball end mill.

### 3.3. TRAJECTORIES DISTRIBUTION: DISTANCE BETWEEN TOOL PATHS AT THE LEADING EDGE

To obtain machining peaks with constant height on a plan, a constant tool path distance has to be maintained. On a complex surface, this is not possible considering the curvature variations: the peak height is variable keeping the tool paths distance constant [8]. Nevertheless, to achieve a comparative study of foil surfaces, a common reference point is chosen. It corresponds to the respect of a constant height at the leading edge. The leading edge is a particular line in hydrodynamics, it is the flow separation line at an incidence angle of zero. The leading edge corresponds to the zone of a stronger variation of curvature. Furthermore it is the easiest zone to compare each foil to each other by neglecting their dimensions. To consider the constant height of machining peaks at the leading edge on an elliptic foil, it is necessary to calculate the distribution of the distance between the tool paths.

The data to calculate the distance for an ball end mill on an elliptic foil (Fig. 3) are: the maximal chord of the foil ( $r_1$ ); the span of the foil ( $r_2$ ); the tool radius ( $R_{\text{tool}}$ ); the position of the first point on the leading edge; and the maximal height of machining peaks ( $h$ ).

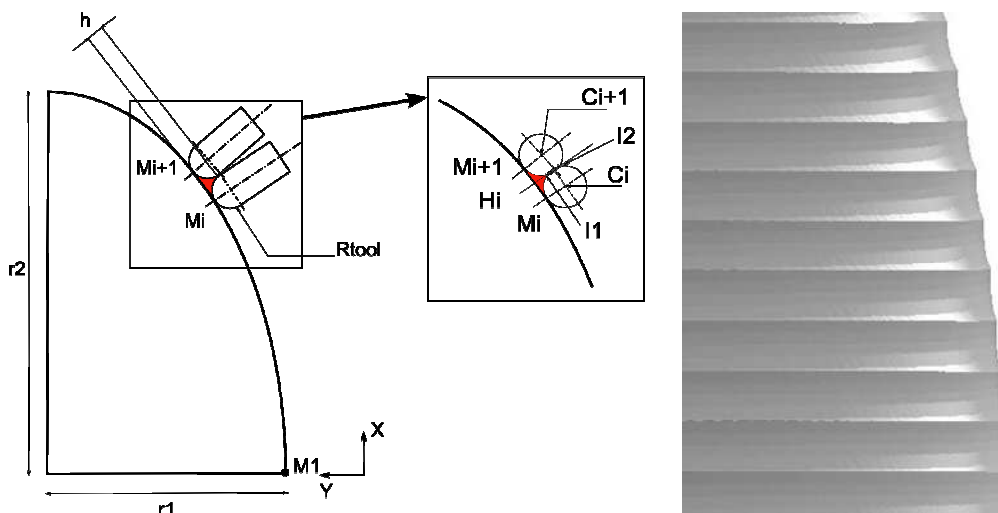


Fig. 3. Computation of the distribution of the distance between tool paths and machining peaks visualisation

The reference foil has an elliptic leading edge, whose geometrical definition is given by semi minor axis  $r_1$  and semi major axis  $r_2$ . The purpose of the computation is to determine the successive  $M_i$  point positions so that the given machining peaks height is equal to the distance  $h$  between the ellipse and the intersection  $I_1$  and between the circles (centres  $C_i$  and  $C_{i+1}$ ) generated by two successive tool paths with a ball end mill ( $R_{\text{tool}}$ ). For the foil n°2, the coordinates of points allow straightly the computations of the different sections composing the trajectory. The coordinates of points calculated for the distribution of distances between tool paths correspond to the coordinates of the particle releases (§ 2.4) for the foil n°3. These particle releases allow to obtain the streamlines that are going to be used for the trajectory generation.

### 3.4. STREAMLINES COMPUTATIONS

In order to simulate the flow of the fluid and to obtain the associated streamlines, the computation domain corresponds to the test section of the hydrodynamic tunnel. The velocity field is calculated for a given incidence angle of  $10^\circ$  to maximize the three-dimensional effects. A upstream flow velocity of  $12 \text{ m}\cdot\text{s}^{-1}$ , is similar to a  $10^6$  Reynolds number. Moreover, the geometrical configuration of the test section is modelled to take into account the blockage effects.

Computation is conducted with the Reynolds Averaged Navier Stokes Equations (RANSE) based code Ansys CFX® which represents the Navier Stokes equations in case of an incompressible and isothermal flow. Particles of the mesh volume are propagated in the velocity field for release points computed in paragraph 2.3. The maximal peak height at the leading edge is set to  $h$  equal to  $0.22\text{mm}$ . The positions of particles in the flow are calculated with an iterative method from the velocity field. Particles are released in the first element of the boundary layer at the leading edge (Fig. 4), to allow the computation of streamlines on the suction side (Fig. 5).

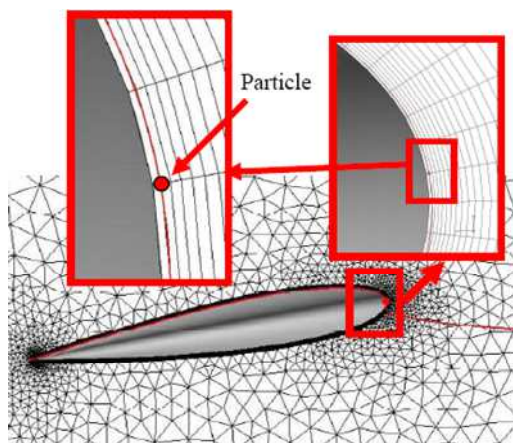


Fig. 4. Release of particles in the first element of boundary layer

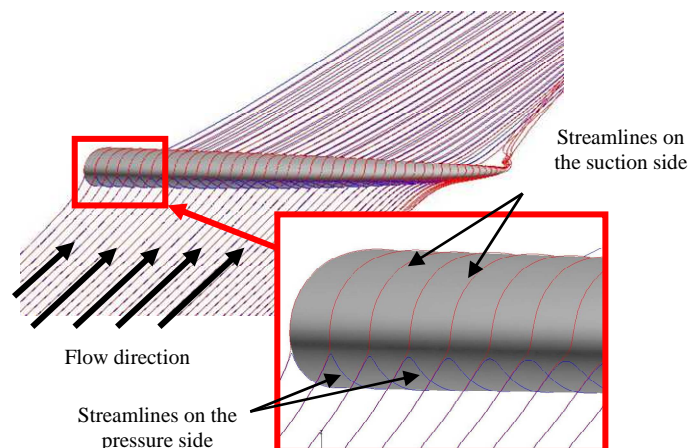


Fig. 5. Streamlines on the pressure side and suction side simulated by Ansys CFX®

## 3.5. TRAJECTORIES GENERATION

Machining tool paths are generated from streamlines stemming from Ansys CFX<sup>®</sup> software. As the computations are different for the streamlines of the pressure side and those of the suction side, two distinct sets of points are treated with CAD software. Then, sets of streamlines are interpolated by using a smoothing method.

An important step during the generation of tool trajectories consists in achieving a continuous trajectory around the foil. So, the streamlines must be connected at the leading and trailing edges.

A join of tangent continuity is created on the leading edge between the suction side streamline and the pressure side streamline (Fig. 6). The curvilinear averaged distance for joins is about 2.7 mm for a 80 mm chord.

The following step consists of connecting the streamlines at the trailing edge (Fig. 7). A connecting curve allows within the manufacturing framework to establish a continuous machining trajectory and to avoid displacements.

In a last step are assembled all the streamlines to generate a continuous trajectory all over the foil. This continuous trajectory is used as a guide for the CAM step as the tool has to follow guide curve to machine defined streamlines.

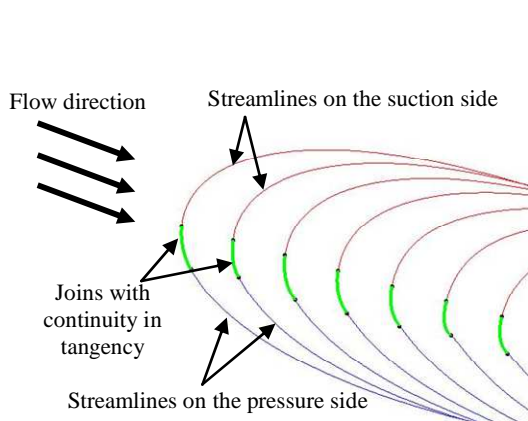


Fig. 6. Joining with tangent continuity between the streamlines of the suction side and the streamlines of the pressure side

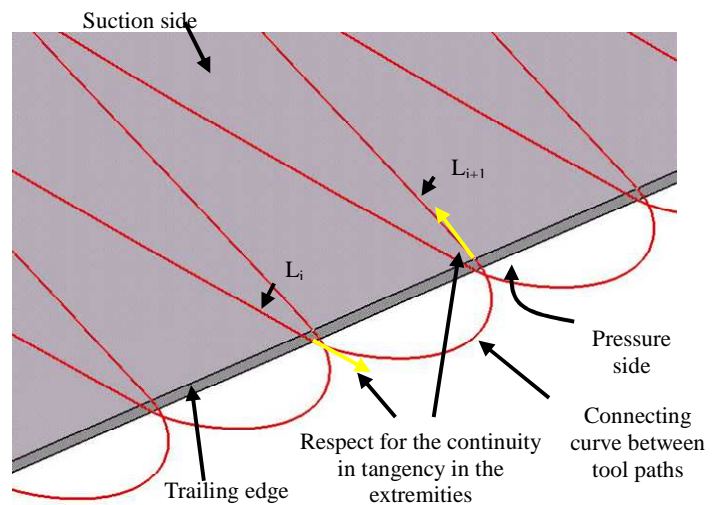


Fig. 7. Connecting curve at trailing edge

### **Particular case : foils n°1 and 2:**

- Foil n°1 has a surface texture like a mirror. A classical manufacturing process is used to machine this foil.

- Foil n°2 has machining peaks parallel to the upstream flow. The distribution of the distance between tool paths is computed for a 0.22 mm maximal peak height at the leading edge. Point coordinates allow a continuous computation of the different sections.



### 4. MANUFACTURING PARAMETERS

Three foils are machined on a 5 axis machining center to achieve the comparative study of the hydrodynamic efforts. The presented manufacturing range concerns only the finishing cut sequence of the foil. The foil corresponds to the functional part of the work piece from a hydrodynamic point of view. To measure the hydrodynamic performances and to machine the foil, it is necessary to clamp it. To clamp the foil, an additional clamping fixture was design (Fig. 8). Some surfaces of this clamping fixture are used as positioning references for the foil. As the hydrodynamic measurements will take place in water environment, the used material has to be resist-proof to resist to corrosion. The material also has to resist to mechanical stresses generated by the hydrodynamic efforts. Thus the chosen material is 304L stainless steel.

#### 4.1. MANUFACTURING RANGE

To allow a continuous machining all over the foil, a setup work-piece is manufactured (Fig.9). In the setup work-piece, the raw machining is oriented thanks to two pawns and it is fixed with a clamping flange. A ball end mill is used to machine the foils with the cutting parameters named in Table 1.

Table 1. Cutting parameters for stainless steel 304L with a carbide ball end mill

Ball end mill	D=16 mm
Vc (m/min)	250
N (tr/min)	5000
F (mm/min)	2000

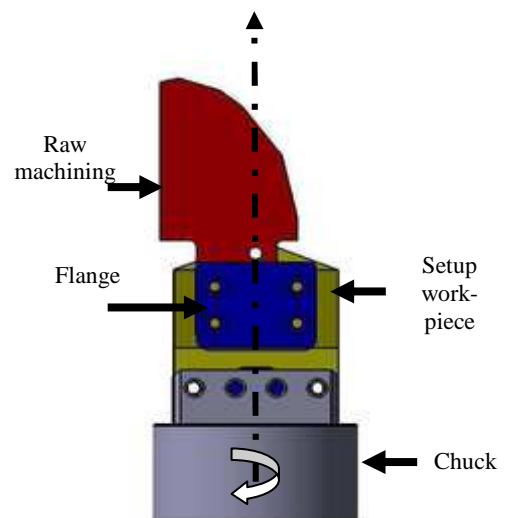
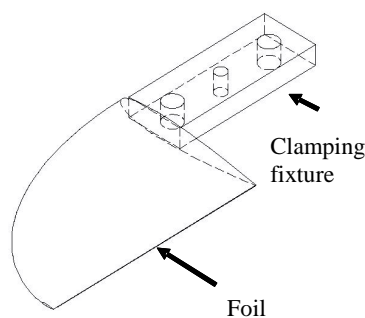


Fig. 8. Work piece design

Fig. 9. Set up and clamping in the setup work-piece

#### 4.2. MACHINING STRATEGIES AND COMPUTER-AIDED DESIGN

CATIA® CAD software allows to carry out the foil modelling and to generate the machining tool paths on a machining center. The trajectories presented in the paragraph 0 are used as a guide to define the machining tool centre paths. To maintain right cutting

conditions and to manage stronger curvature variation, the tool must be tilted throughout the tool trajectory. The chosen lead and tilt angles relative to the normal of the foil shape surface are presented in Fig. 10 and their values are given in Table 2.

Table 2. Lateral and frontal slopes values

Name of the foil	Frontal slope angle ( $\gamma$ )	Lateral slope angle ( $\beta$ )
Foil n°2	15°	0°
Foil n°3	1° to 20°	0° to 10°

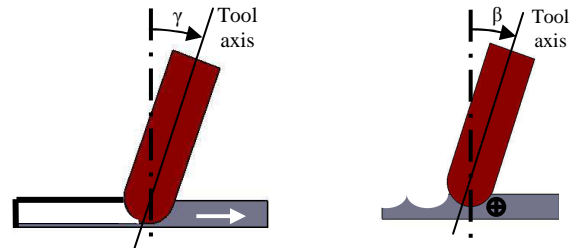


Fig. 10. Lateral and frontal slope angles

#### 4.3. EQUIPMENT: 5 AXIS MACHINING CENTRE

The machining is performed using the 5 axis machining center: Turbomill 1200 from Liechti. This type of machine is dedicated for the manufacturing of turbine blades. It is adapted to the manufacturing of the studied foils because of the continuous rotation of the  $\bar{A}$  axis on which the work piece is located. This 5 axis machining center kinematic allows the tool to bypass the foil in a continuous way. The 5 axis machining center is configured as the following: axes linked to the spindle:  $\bar{X}$ ,  $\bar{Y}$ ,  $\bar{B}$ ,  $\bar{Z}$ , axis linked to the foil with no machine table:  $\bar{A}$ .

#### 4.4. MACHINING OPERATING STEPS

The manufacturing of foils n°2 and 3 were achieved according to the presented. Fig. 11 illustrates the main steps from conception until machining: trajectories generating, machining tool paths generation, machining tool paths validate and finally the foil machining result.

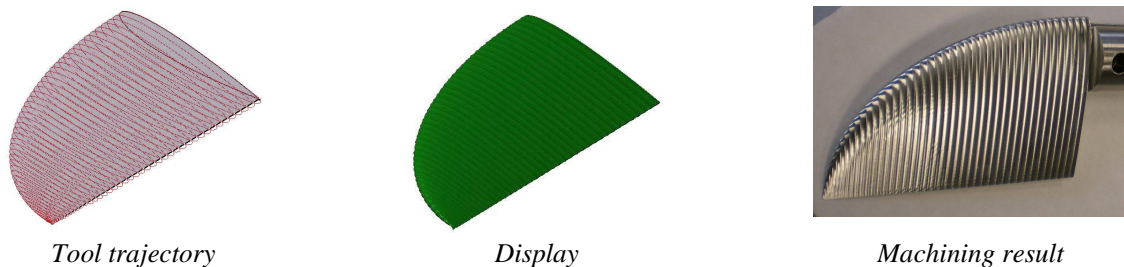


Fig. 11. Example : illustrations of the main manufacturing steps of foil n°2



## 5. HYDRODYNAMIC TESTS

### 5.1. PRESENTATION OF THE HYDRODYNAMIC COEFFICIENTS

The hydrodynamic efforts generated on a foil by a flow are lift, drag and torque. The measurement system has two coordinate systems which are presented in Fig. 12. The first coordinate system is fixed ( $xOy$ ), corresponds to the tunnel test section reference as its  $x$  axis corresponds to the upstream flow direction. The second coordinate system ( $x'Oy'$ ) is linked with the foil, and the foil angular position corresponds to the incidence angle ( $\alpha$ ), in regard to the fixed coordinate system ( $xOy$ ).

In the tunnel test section, drag  $F_X$  is the resistance effort applied by a fluid on an object. This effort  $F_X$  is parallel to the upstream flow. The lift effort,  $F_Y$ , is a perpendicular effort of the upstream flow direction. It is created by the suction in a zone of low pressure formed on the suction side of the foil. The computation of dimensionless hydrodynamic coefficients allows to compare the foils hydrodynamic performance.

Data:  $C_D$ : drag coefficient;  $C_L$ : lift coefficient;  $V_\infty$ : upstream flow velocity (m.s-1);  $\rho$ : flow density ( $\text{m}^3/\text{kg}$ );  $S$ : planned surface ( $\text{m}^2$ )

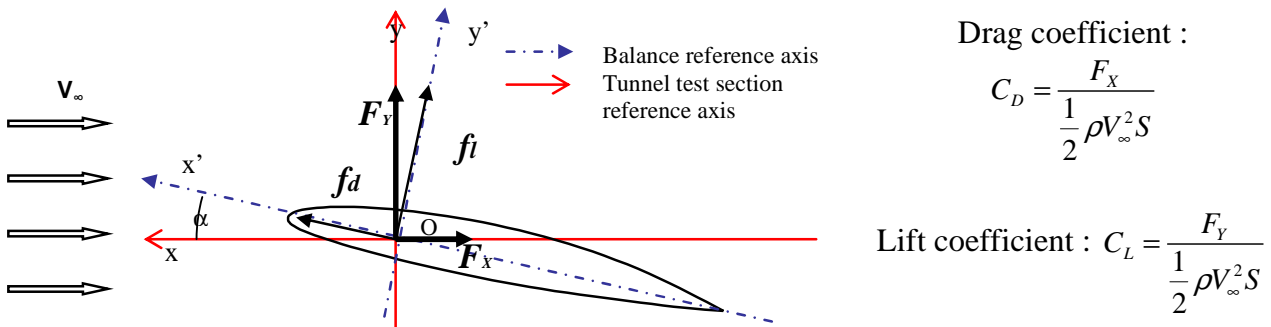


Fig. 12. Coordinate systems definition

### 5.2. EXPERIMENTAL SETUP

Measurements are carried out in a hydrodynamic tunnel. During the experiments, drag and lift efforts are measured in given operating conditions: the fluid pressure  $P$ , the flow velocity  $U$  and the incidence angle ( $\alpha$ ). The incidence angle ( $\alpha$ ) is measured between the foil chord direction and the upstream flow axis (Fig 12). It allows to control the fluid velocity range between 0 and 15 m.s-1 and pressure in the test tunnel range from 30 mbar to 3 bars. The foils are located in the test section and can be rotated to obtain the desired incidence angle ( $\alpha$ ). The foils are clamped in a three components sensor, “hydrodynamic balance” based on deformation gauges to measure the lift and drag efforts (Fig. 13).

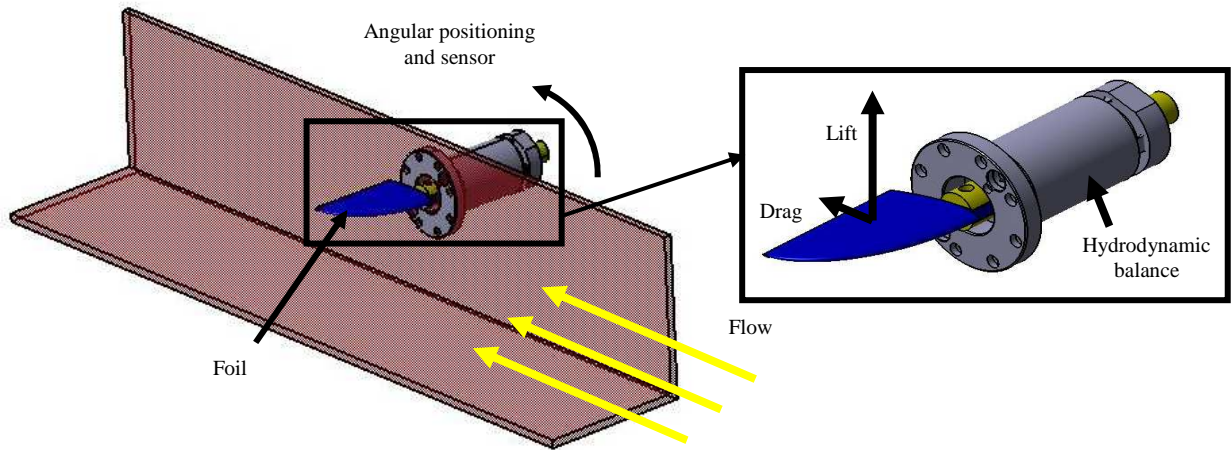


Fig. 13. Scheme of a foil in the test section of the hydrodynamic tunnel and foil clamped in the hydrodynamic balance sensor

### 5.3. HYDRODYNAMIC RESULTS

Measurements are carried out for upstream flow velocity  $V_\infty$  up to 12 m.s<sup>-1</sup> as during the computations and the incidence angle ( $\alpha$ ) range from  $-15^\circ$  to  $15^\circ$ . To avoid cavitation phenomena, the pressure in the tunnel is set to 1450 mbar. Signal are sampled at a frequency of 4096 Hz, corresponding to 122880 measured points in 30 seconds. The presented results correspond to an average of raw measures. This achieved data is averaged before calculating the coefficients.

Measurements of the lift  $C_L$  and drag  $C_D$  coefficient according to the incidence angle ( $\alpha$ ) are presented in Fig. 14 and Fig. 15.

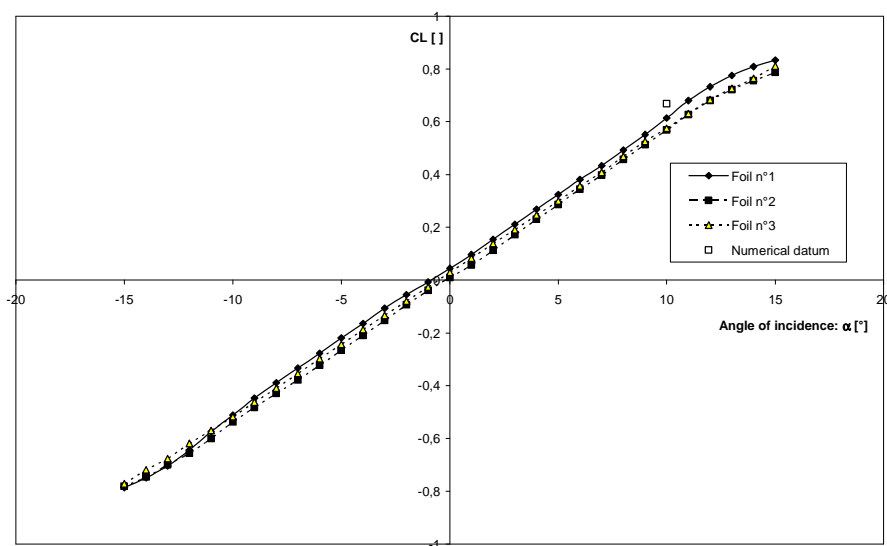


Fig. 14. Variation of the lift coefficient according to the angle of incidence for the 3 foils

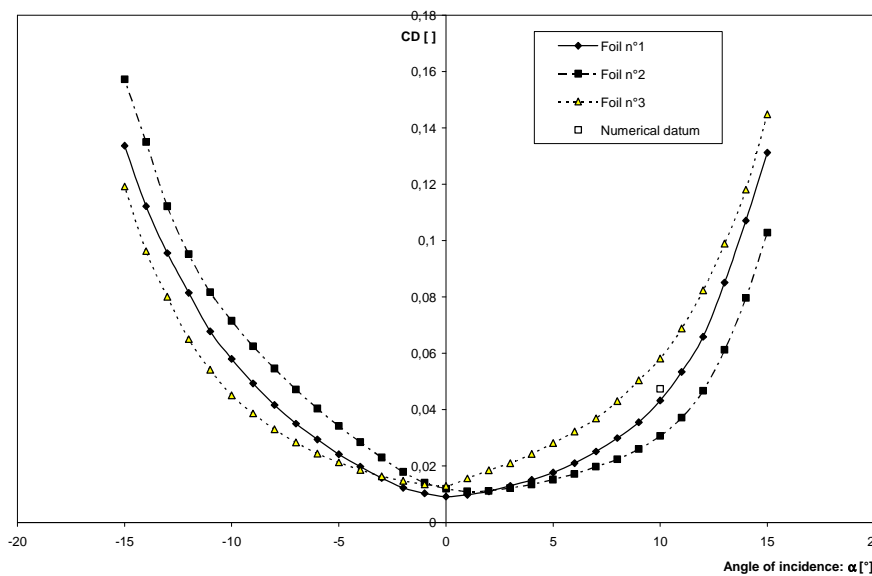


Fig. 15. Variation of the drag coefficient according to the angle of incidence for the 3 foils

Fig. 14 shows that the lift coefficient  $C_L$  increase linearly according to the incidence angle ( $\alpha$ ) for the three foils. For foils n°2 and 3, the lift coefficient value is equal to zero at an incidence angle of zero degrees. Looking at the foil n°1, the lift coefficient value is equal to zero for an incidence angle of 1°. This gap can be due to an angular offset about the positioning of the foil or to a geometric dissymmetry of the foil. For foil n°1, the  $C_L$  curve is not symmetric regarding to the incidence angle of 0°. For the three foils, a curve inflection is observed at an angle of 10°.

Fig. 15 shows that the behaviour of the three foils differs in regards to the drag coefficient  $C_D$ . Drag coefficient curves of the 3 foils are not symmetric with regard to the Y axis. For foils n°1 and 3, the drag coefficient is minimal for an incidence angle of 0°. For foil n°2, the minimum drag coefficient is located at an incidence angle of 1°.

## 6. DISCUSSION

In this passage on the one hand the analysis of hydrodynamic results are discussed, the curve observations being detailed in the paragraph 0, and on the other hand, the link between the manufacturing of a given surface texture and its cost (duration, preparation ...).

The lift coefficient for the three tested foils increases linearly according to the incidence angle  $\alpha$  on an angular range from -10° to 10°. This behaviour corresponds to the classic variation of the lift coefficient of a symmetric foil. Below  $\alpha = -10^\circ$  and above  $\alpha = 10^\circ$ , a curve inflection corresponding to the beginning of the lift fall is observed.

For a symmetric tested foil, a current usage consists in displacing the  $C_L$  and  $C_D$  curves. The zero position value of the lift coefficient is demanded for an angle of incidence of 0°. This readjustment is made for compensating the defects linked with the experimental protocol as the angular uncertainties during the positioning of the foil. As foil n°3 is not

symmetric; in this case, the hydrodynamic coefficients cannot be and are not readjusted, and the only raw data is compared.

To vary of the drag coefficient, the curve is only supposed to be symmetric for the symmetric and polished foil n°1. Furthermore we can note that the highest drag coefficient obtained at 10° corresponds to foil n°3, although this foil is manufactured according to the streamlines resulting from a computation for an incidence angle of 10°. Therefore the trajectories are optimised for this incidence angle.

For the incidence angle of 10°, analysis of the lift and drag curves allows to conclude that the surface texture of the foils influence less the lift coefficient, 7% difference, than the drag coefficient, 30% difference.

Besides the surface texture influence on hydrodynamic performances, it is also necessary to take into account the design and machining durations according to the desired surface texture.

Table 3. Machining duration of the finishing sequence for each foil

	Machining duration (min)
Foil n°1	210
Foil n°2	28
Foil n°3	24

The design of foil n°1 requires a CAD software, and for the generation of the machining tool paths a classical CAM approach. Then for foil n°2, it is necessary to calculate at first the distribution of the distances between tool paths at the leading edge and secondly to generate the trajectory from sections and from connecting curves allowing to obtain a continuous trajectory. Finally, for foil n°3, the software chain becomes more complex, it involves five different softwares before obtaining the trajectories.

To conclude, for an incidence angle of 10°, foil n°2 seems to deliver the best compromise. It has the best hydrodynamic performances, that is the weakest drag coefficient, and conception and manufacturing durations are less complex in comparison to the other foils (Table 3).

## 7. CONCLUSION AND PERSPECTIVES

The purpose of this study is to take into account the constraints and criteria of hydrodynamics applied to design for manufacturing. To achieve the presented foils, this multidisciplinary method takes hydrodynamic constraints and manufacturing constraints into account. A compromise between the hydrodynamic performances and the manufacturing cost in the context of design for manufacturing is needed. To find this compromise, three foils are machined and their hydrodynamic performances are compared. The first foil is achieved through a classic manufacturing process, the second is manufactured considering hydrodynamic characteristic data and finally the third is

manufactured considering flow characteristic data. For the machining of each foil, several parameters are respected: no recovery zone, predefined peak height at the leading edge and continuous machining tool paths. Analysis of the results showed that foil n°2 has the best performances for a ten-degree incidence angle, and furthermore its manufacturing durations are reduced. Thus, the manufacturing of foils with machining peaks parallel to the upstream flow seems to be the best compromise to meet machining and hydrodynamic requirements.

Drawing from these results, there are prospects for several further studies, in particular the influence of the roughness inside the machining grooves, the influence of the positioning defects in the hydrodynamic balance and the influence of the machining direction.

#### ACKNOWLEDGEMENTS

This work was supported with a special research fund from the regions of Bretagne and Pays de la Loire. This work was carried out within the context of the working group Manufacturing 21 (17 French research laboratories). The topics approached are: modeling of the manufacturing process, virtual machining, emerging manufacturing methods.

#### REFERENCES

- [1] CARLTON J.S., *Marine Propellers and Propulsion*, Butterworth Heinemann Ltd, ISBN 075061143X, 1994, 432.
- [2] BRIENT A., LEROUX J.B., MARTINEAU J.P., ASTOLFI J.A., HASCOËT J.Y., *An Experimental Analysis of the Effect of Roughness Produced by Machining on Hydrodynamic Performance of Two-Dimensional Hydrofoil*, Proceedings of the 3rd International Conference on Navy and Shipbuilding Nowadays, Saint-Petersburg, Russia, 2003, 249-254.
- [3] SVENSEN E., MEDHURST J. S., *A Simplified Method for the Assessment of Propeller Roughness Penalties*, Marine Technology, Vol. 21, No. 1, 1984, 41-48.
- [4] ISO 484/1., *Hélices de navires – Tolérances de fabrication – Partie 1 : Hélices de diamètre supérieur à 2,50 m*, NF J 65-510, Décembre 1985.
- [5] DAMAY T., JAOUEN R., HASCOËT J.Y., MARTINEAU J.P., BRIENT A., ASTOLFI J.A., HAUVILLE F., 2007. - *Design for Manufacturing applied to Hydrofoils dedicated to Marine Propellers* - Proceedings of sixth International Conference (2007) on High Speed Machining, San Sebastian, Spain, 21-22 Mars, 2007, 432-437.
- [6] FRUMAN D. H., CERRUTI P., PICHON T., DUPONT P., *Effect of Hydrofoil Planform on Tip Vortex Roll-Up and Cavitation*, J. Fluids Eng., Volume 117, Issue 1, 1995, 162 (8 pages).
- [7] RAMOS A. M., RELVAS C., SIMÕES J. A., *The influence of finishing milling strategies on texture, roughness and dimensional deviations on the machining of complex surfaces*, Journal of Materials Processing Technology, Volume 136, Issues 1-3, 10 May 2003, 209-216.
- [8] BOUJELBENE M., BRENIER B., FABRE A., MOISAN A., *A contribution to the improvement of surface texture for die and mold machining*, Proceedings of the 4th International Conference on Integrated Design and Manufacturing in Mechanical Engineering, Clermont-Ferrand, France, 2002, 10.